



## Estimation of tire-road friction coefficient for improving the engagement control of automotive dry clutch

Abbas Soltani<sup>1\*</sup>, Milad Arianfard<sup>2</sup>

<sup>1</sup>Department of Industrial, Mechanical and Aerospace Engineering, Buein Zahra Technical University, Qazvin, Iran.

<sup>2</sup>Department of Mechanical Engineering, Technical and Vocational University (TVU), Tehran, Iran.

### ARTICLE INFO

#### Article history:

Received : 5 May 2022

Accepted: 9 Jun 2022

Published: 29 Jun 2022

#### Keywords:

Clutch engagement control

Parameter estimation

Road friction coefficient

Adaptive sliding mode control

Unscented Kalman filter

### ABSTRACT

An adaptive sliding mode controller (ASMC) based on estimation of tire-road friction coefficient is proposed for engagement control of automotive dry clutch. The control of clutch engagement is one of the most important parts of gear-shift process for automated manual transmission. Accurate amount of drive shaft torque in modelling of powertrain system is essential to guarantee smooth engagement of the clutch and rapid response of the control system. As the tire-road friction coefficient has significant influence on drive shaft torque, an estimator is designed to calculate this parameter. The ASMC is proposed for the clutch control to overcome the system uncertainties and a proportional integral (PI) controller is adopted to engine speed control. In addition, an estimator based on an unscented Kalman filter is used to observe the states hardly measured like wheel slip ratio and longitudinal vehicle velocity. The simulation results show the significant capability of the combined use of the designed control system and road friction coefficient estimator for improving the smooth clutch engagement in comparison to the control system without estimator.

## 1. Introduction

An automated manual transmission (AMT) contains two actuators for the clutch control engagement and the gear shifting process. Smooth synchronization of engine and clutch input shaft is achieved by proper design of clutch engagement controller. If the performance of the controller is not excellent, it causes oscillations in the powertrain and uncomfortable driving [1-3].

One of the most sophisticated parts of the design for the AMT system with dry clutch is the launch control of a vehicle from the standstill. Because, the proposed control approach should ensure the small dissipated work due to the clutch slip and also, the smooth and fast engagement of the clutch without fluctuations by controlling the normal

clutch force and engine torque, at the same time. Therefore, the engagement control of the dry clutch, especially when vehicle starting, is a crucial process to minimize the facing wear and to perform the driveline efficiently. A control system of dry clutch engagement was designed for vehicle launches using a shaft torque observer. The observer included two parts, stick phase and slip [4].

To enable smooth clutch engagement control, the method of dynamic programming was utilized to compute the engine torque value during clutch engagement [3]. As the frictional torque of the dry clutch changes during a long period of time, a robust H-infinity controller was adopted to design a precise model to cope with model uncertainties and system disturbances due to the effects of long-

\*Corresponding Author

Email Address: [soltani@bzte.ac.ir](mailto:soltani@bzte.ac.ir)

<https://doi.org/10.22068/ase.2023.642>

time wear or temperature changing [5]. Gao and et al. designed a clutch disengagement approach to control the AMT. The control strategy was proposed based on an observer of drive shaft torque [6].

A strategy of control for engine constant speed was presented in the vehicle launching and gear shifting operation, based on the dynamic modeling of the powertrain system. The desired and real values of the engine speed were restricted via controlling the clutch in the vehicle launching [7]. The engagement of the clutch for an AMT system was proposed by using optimal control. The clutch friction force and the vehicle powertrain variables were estimated using an adaptive observer [8].

An optimal tracking control was put forward for vehicle dry clutch. The tracking problem was derived and analyzed through the torque values of the clutch and engine [9]. A controller was developed for gearshift and clutch engagement in AMTs which applied the models for the driveline, dry clutch and electrohydraulic actuator [10]. An investigation on the control of smooth clutch engagement illustrated that the significant results could be achieved for the vehicle launching control without any shock by pneumatic clutch actuators [11]. An accurate model of the power transmission of a heavy truck with AMT was designed. It took into account both the dynamics of the transmission shafts, and the servo-actuated clutch and gearbox. The researchers investigated the influences of the pneumatic actuators on powertrain action and on longitudinal vehicle dynamics [12].

The value of drive shaft torque affects the operation of longitudinal vehicle dynamic. A shaft torque estimator was designed for the automotives with stepped ratio transmissions. Model uncertainties and the unmodeled dynamics were taken into account as disturbances of the system [13, 14]. It is also well known that hill start control is one of the main systems for the AMT. The control algorithm of the hill start is a little more complicated in comparison to the other control systems of transmission [15]. The researchers proposed a force and position control for the gear shifting process which had multi phases with nonlinear specifications [16]. A robust controller based on combined application of a sliding mode controller (SMC) and a PID control was designed for a clutch-by-wire actuator in the vehicle applications [17].

Song et al. [18] investigated a new power transmission controller for longitudinal dynamic control of an AMT. By using the system, the

vehicle accurately followed the motion with positive or negative acceleration. In [19], an electrohydraulic AMT of a three-wheeled motorcycle was studied. An electrohydraulic clutch actuator was replaced by a novel electromechanical clutch actuator to cope with fuel wasting utilizing a SMC.

In the performed researches, the states of the AMT were taken into account as the measurable variables, while some states such as longitudinal vehicle velocity, wheel slip ratio and the clutch torque cannot be measured easily. Therefore, in the practical applications, the noticeable errors will be appeared in the performance of the clutch control system. So, it will be needed to estimate the mentioned states precisely. The torque is transmitted from the engine to the drive shaft through the clutch, and the drive shaft torque is extremely dependent on the road friction force. Consequently, its variations are significant. Therefore, an estimator of road friction coefficient should be proposed, whereby the clutch torque can be accurately observed in real-time. With regard to the estimation issue, an unscented Kalman filter (UKF) was applied to observe the states of a vehicle model with seven degrees of freedom (DOF) [20]. In addition, a real-time estimator was proposed to observe the clutch torque specifications of a clutch model. In this work, the model uncertainties were considered [21].

Dry clutch is widely used in vehicle transmissions because of their reliability and efficiency paired with low fuel consumption and reduction of pollutant emissions. A prerequisite to attain these goals in automated manual transmissions is the adoption of a “good” clutch model and the design of a robust control strategy. Several papers have been dedicated to modeling and engagement control of dry clutches, both in mechanical and control engineering literature. An overview of dry clutch torque modeling was proposed together with a discussion on the main factors which affect the torque transmission [22].

An automotive transmission system equipped with electronic or electrohydraulic actuators, controlled by an electronic control unit, provided clutch-less driving experience to the driver for the shifting operation. [23].

By studying the literature review, the major novelty of this study is the design of an ASMC associated with the UKF and the estimation of the road friction force to enhance the smooth clutch engagement in comparison to the control system without estimator. The longitudinal vehicle

velocity, slip ratio of the wheel, and the clutch torque are estimated utilizing the UKF. Moreover, the road friction forces are observed based on the Pacejka tire model.

Accordingly, in the second section of paper, a dynamic model of the vehicle powertrain with three DOF is presented. The Pacejka tire model is applied for simulation of longitudinal vehicle dynamics. In section three, the UKF and the estimation algorithm of road friction force are explained. In the next section, the control of clutch engagement is discussed via the ASMC. The operation of the presented controller for the clutch is discussed with some simulations in the fifth section. Conclusions are provided in section 6.

## 2. System dynamic modelling

In this part, the dynamic equations of the powertrain system, longitudinal vehicle dynamic, engine output torque and the tire-ground force are modelled.

### 2.1. powertrain model

The powertrain model should be modelled in order to consider all the dynamics of the system, and also simple enough to be easily implemented in commercial electronic control units. The powertrain system of a vehicle with an AMT is illustrated in Figure 1. The model of the driveline system contains the engine, the clutch and the longitudinal dynamics and utilized to present the flow of the torque from the engine to the tires can be depicted as Figure 2.

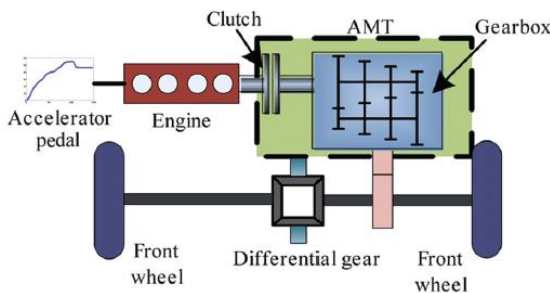


Figure 1: The powertrain system of a vehicle with the AMT [24]

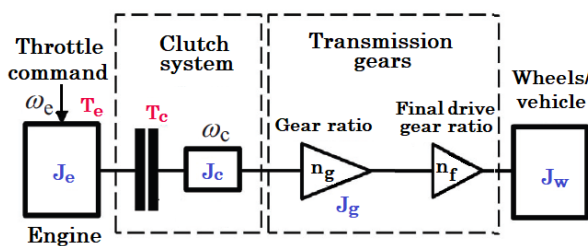


Figure 2: Simplified driveline model

When the engine flywheel and the clutch disk are in slipping operating conditions during vehicle launching, the driveline model with two DOF can be described as follows:

$$T_c - R_w \frac{F_T}{n} = J_t \frac{d\omega_c}{dt} \tag{1}$$

$$T_e - T_c = J_e \frac{d\omega_e}{dt} \tag{2}$$

$$J_t = J_c + \frac{J_g}{n_g^2} + \frac{J_w}{n^2} \tag{3}$$

where  $J_e$  is the engine inertia,  $J_c$  represents the inertia of clutch and gearbox input shaft and all the rotating inertias related to it,  $J_g$  is the inertia of gearbox output shaft and the rotating inertias connected to it,  $J_w$  denotes the overall inertia rotating with the wheel speed such as wheel, drive shaft and differential,  $J_t$  is the equivalent inertia moment of driveline at the clutch from the wheels to the clutch,  $T_e$  is the engine torque,  $T_c$  is the clutch torque,  $\omega_e$  and  $\omega_c$  are the engine rotational speed and the clutch speed respectively,  $R_w$  is wheel radius,  $F_T$  is the traction tire-ground force,  $n_g$  is the gear ratio,  $n_f$  is the differential ratio,  $n$  is the overall gear ratio equals to  $n_g \times n_f$ . This model is sufficiently simple to be applied for proposing the clutch controller when the vehicle launching. At the same time, the main dynamics of the powertrain are considered. Also, the stiffness coefficients of all the transmission shafts are neglected.

### 2.2. Longitudinal vehicle dynamic model

Equation of longitudinal vehicle dynamic model with one DOF on a road without slope by ignoring the aerodynamics resistance force can be derived as:

$$F_T - mgf_r = m \frac{dv}{dt} \tag{4}$$

where  $m$  is the vehicle mass,  $v$  is the vehicle speed and  $f_r$  represents the rolling resistance coefficient of the tire.

### 2.3. Tire model

The Pacejka tire model has been utilized to compute the tire forces. Since in this study, only the longitudinal motion of the vehicle is considered, the lateral forces of the tire model are not obtained. The Pacejka tire model is described by following equations:

$$F_T = \mu D_x \sin [C_x \arctan (B_x \phi_x)] \tag{5}$$

$$D_x = \mu (a_1 F_z^2 + a_2 F_z) \quad (6)$$

$$B_x = (2 - \mu) \left( \frac{a_3 F_z^2 + a_4 F_z}{C_x D_x e^{a_5 F_z}} \right) \quad (7)$$

$$E_x = a_6 F_z^2 + a_7 F_z + a_8 \quad (8)$$

$$\phi_x = (1 - E_x)\lambda + \frac{E_x}{B_x} \arctan (B_x \lambda) \quad (9)$$

$$\lambda = \frac{R_w \omega_w - v}{\max (R_w \omega_w, v)}, \quad (\omega_w = \frac{\omega_c}{n}) \quad (10)$$

where,  $a_1$  to  $a_8$  are the empirical coefficients of tire [20],  $C_x = 1.65$ ,  $\omega_w$  is the rotational wheel speed and  $\lambda$  denotes the longitudinal wheel slip ratio.

### 2.4. Engine model

It is very difficult to present a very detailed engine model. Because there is combustion, thermodynamics, friction, etc. inside the engine which have hard non-linearity characteristics. The stable state output torque of an engine can be expressed as a function of the engine speed  $\omega_e$  and the throttle opening  $\beta$  as follows:

$$T_e = f(\omega_e, \beta) \quad (11)$$

This research uses the experimental data to represent the model of an EF7 engine. The engine output torque in the simulation is found by the EF7 engine torque map, Figure 3, which is a look-up table with the engine speed and the throttle as inputs and the engine torque as output.

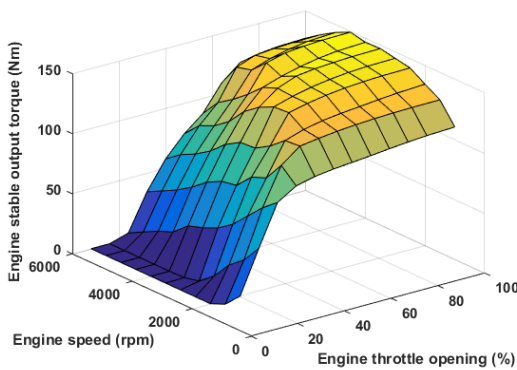


Figure 3: The EF7 engine torque map [25]

### 3. Design of the estimator

The state variables are estimated using the UKF. afterward, the road friction coefficient is estimated

using the estimated variables and equations of the tire model.

### 3.1. Estimation of the states using the UKF

In this research, the states of the longitudinal vehicle velocity, slip ratio of the wheel, engine speed and also the clutch torque, are estimated using the UKF. It is noticeable, that the wheel rotational speed and longitudinal vehicle acceleration are the measurable variables. The state variables are:

$$x = [v, \lambda, \omega_e, T_c]^T \quad (12)$$

The non-linear state-space model can be expressed as follows [1]:

$$x_{k+1} = f(x_{k+1}, u_k, t_k) + w_k \quad (13)$$

$$y_k = h(x_k, t_k) + v_k \quad (14)$$

Where  $f$  is the vehicle system dynamics,  $x_k$  and  $t_k$  are the state and time at the sampling instant  $k$ ,  $u_k$  is the input to the system at the sampling instant  $k$ ,  $y_k$  is a set of noisy measurements determined by function of  $h$ .  $w_k$  is the process noise, while  $v_k$  is the measurement noise. The added noises are assumed to be normally distributed Gaussian white noises with zero mean whose covariance matrices are  $Q$  and  $R$ , respectively.

### 3.2. Estimation of the road friction coefficient

The road friction force estimation in practical applications is very significant for accurate accelerating or decelerating performance. In this paper, the road friction force is estimated using the longitudinal vehicle dynamic equation.

First, by the measured vehicle acceleration  $a_x$ , the estimated slip ratio  $\hat{\lambda}$ , rolling resistance of the tire  $f_r$ , and the factors  $B_x$ ,  $D_x$ ,  $E_x$  of the Pacejka tire model, the values of  $\hat{F}_T$  and  $\hat{\phi}_x$  should be computed. Thereafter, the tire-road friction coefficient  $\hat{\mu}$  is obtained using (17).

$$F_T = m(a_x + g f_r) \quad (15)$$

$$\phi_x = (1 - E_x) \hat{\lambda} + \left( \frac{E_x}{B_x} \right) \arctan (B_x \hat{\lambda}) \quad (16)$$

$$\hat{\mu} = \frac{F_T}{D_x \sin [C_x \arctan (B_x \phi_x)]} \quad (17)$$

### 4. Design of the clutch control

The system control is proposed through ASMC for smooth engagement of clutch in this part. It can be observed that the powertrain fluctuations

depend on the rate of change for the clutch slip speed  $\omega_s = \omega_e - \omega_c$  in terms of time at the engagement.

First, the SMC is presented in which, the error functions are given as follows:

$$e = \omega_e - \omega_c = \omega_s \Rightarrow \dot{e} = \dot{\omega}_s \quad (18)$$

The sliding surface  $S$  consists of error and its derivative written as:

$$S = \dot{e} + k_1 e \Rightarrow \dot{S} = \ddot{e} + k_1 \dot{e} = \dot{\omega}_s + k_1 \dot{\omega}_s \quad (19)$$

where  $k_1$  is the strictly positive design scalar. The dynamics of the sliding surface should be considered as follows:

$$\dot{S} = -\eta \text{sign}(S); \quad (\eta > 0) \quad (20)$$

Consequently:

$$\frac{1}{2} \left( \frac{d}{dt} \right) S^2 = S\dot{S} = -\eta \text{sign}(S) S < 0 \quad (21)$$

where  $\eta$  is a positive constant. It can be found using (37) and (38):

$$(\ddot{\omega}_e - \ddot{\omega}_c) + k_1(\dot{\omega}_e - \dot{\omega}_c) = -\eta \text{sign}(S) \quad (22)$$

By differentiating (1), (2) and (4), and combining them with (1), (2) and (22), the SMC control law is given as:

$$u_1 = \dot{T}_c = J_{eq} \cdot \left[ \frac{\dot{T}_e}{J_e} + \frac{R_w m \dot{a}_x}{n J_t} + k_1 \dot{\omega}_s + \eta \text{sign}(S) \right] \quad (23)$$

$$J_{eq} = \frac{J_e J_t}{J_e + J_t} \quad (24)$$

In order to design the ASMC, (19) and (20) are modified as follows:

$$S = \dot{e} + \tilde{k}_1 e \quad (25)$$

$$\dot{S} = -\tilde{\eta} \text{sign}(S) \quad (26)$$

where  $\tilde{k}_1$  and  $\tilde{\eta}$  are the adaptable gains and updated as follows:

$$\dot{\tilde{k}}_1 = \gamma_{y1} |S|; \quad (\gamma_{y1} = 0.01) \quad (27)$$

$$\dot{\tilde{\eta}} = \gamma_{y2} |S|; \quad (\gamma_{y2} = 2.5) \quad (28)$$

In order to keep engine speed constant and avoid the engine stall in vehicle launching, a PI controller is designed. The PI control algorithm is described as following:

$$T_e = k_p \omega_s + k_I \int_0^t \omega_s dt \Rightarrow u_2 = \dot{T}_e = k_p \dot{\omega}_s + k_I \omega_s \quad (29)$$

After finding the output torque of the engine by PI controller, the throttle opening  $\beta$  is obtained by 3-dimension interpolation method and a look-up table based on the EF7 engine torque map whose inputs are the engine torque  $T_e$  and the engine speed  $\omega_e$ . Its output is the throttle opening  $\beta$ . The overall structure for the control of smooth clutch engagement when the vehicle launching is shown in Figure 4.

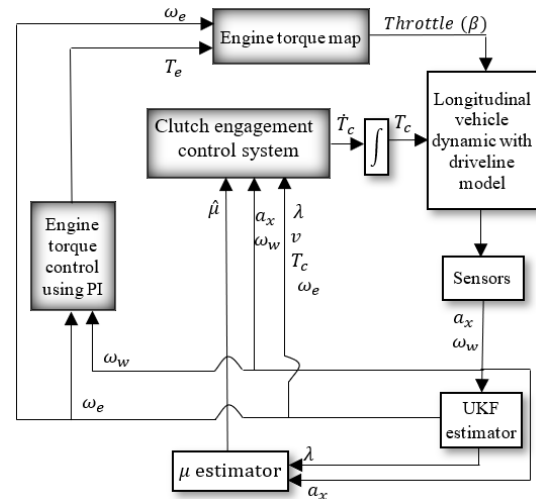


Figure 4: Block diagram of the proposed controller scheme

### 5. Simulation results and discussion

In this section, a longitudinal vehicle dynamic model with driveline modeling is taken into account for analysis. Since there is a conflicting problem between the driving comfort and minimizing the clutch engagement time, both of the issues should be considered to design the clutch controller. The parameters of the vehicle model are listed in Table 1. The initial vehicle speed is equal to zero.

Table 1: Parameter values of the vehicle model

Parameter	Unit	Value	Parameter	Unit	Value
$J_e$	$Kg.m^2$	0.22	$R_w$	$m$	0.3
$J_c$	$Kg.m^2$	0.05	$f_r$	-	0.015
$J_g$	$Kg.m^2$	0.1	$n_{g,1}$	-	3.45
$J_w$	$Kg.m^2$	4.2	$n_f$	-	4.53
$m$	$Kg$	1000	$\mu$	-	0.9

To investigate the accuracy of the controller, without any model uncertainties, to guarantee smooth engagement of the clutch, the rotational speeds of the clutch disk and the engine, and also the estimated values of engine speed with the UKF

(Estimated) can be seen in Figure 5. It is assumed the vehicle runs on a dry road ( $\mu = 0.9$ ). According to this figure, it is obvious that the estimated engine speed quickly converges from an initial value to the real value. Moreover, the clutch engagement time has been reduced. Also, it can be observed that the graphs of the clutch and engine speeds are converged with the same slope, which reduces the driveline oscillations after clutch lock-up. To show this more clearly, the slip speed ( $\omega_s = \omega_e - \omega_c$ ) is plotted in Figure 6. The longitudinal vehicle velocity is illustrated in Figure 7.

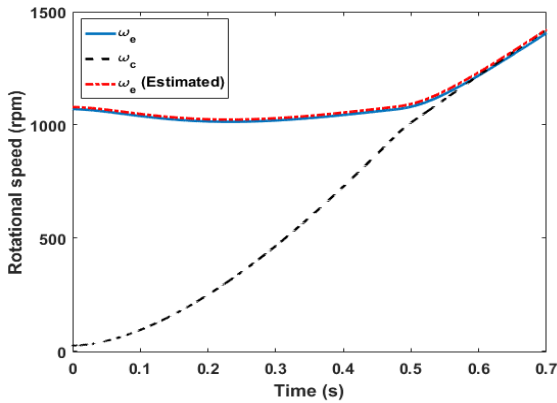


Figure 5: Rotational speed of engine and clutch disk during the engagement

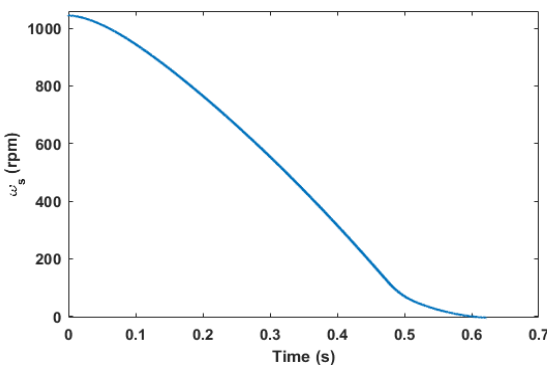


Figure 6: Clutch slip speed

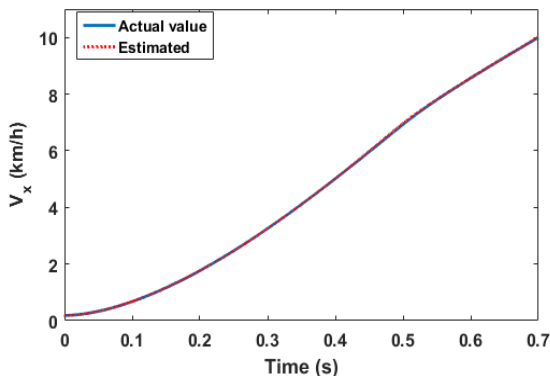


Figure 7: Longitudinal vehicle velocity

The longitudinal vehicle acceleration is shown in Figure 8. The torque values of engine and clutch

during the engagement can be depicted in Figure 9. Figure 10 shows the throttle input obtained through the proposed PI controller.

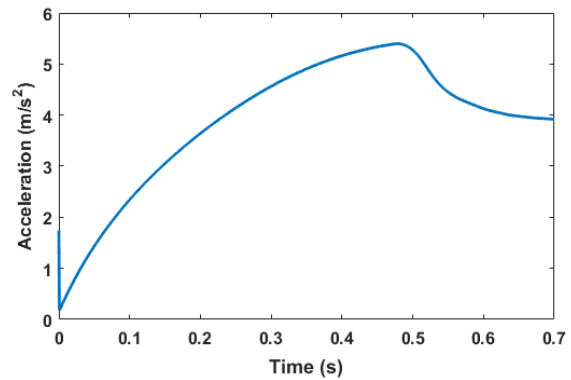


Figure 8: Longitudinal vehicle acceleration

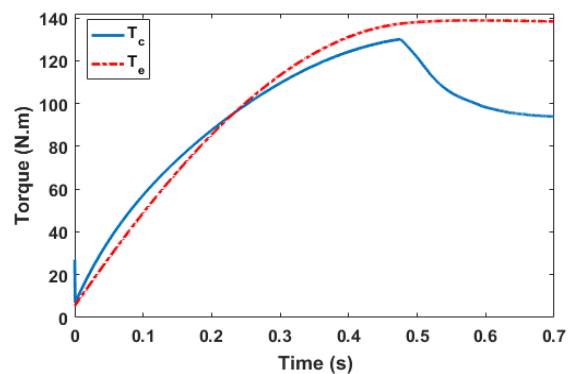


Figure 9: Torque values of engine and clutch

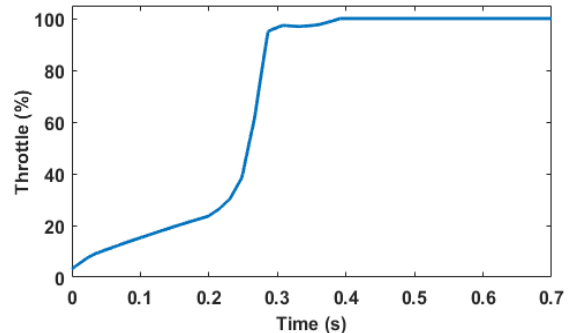


Figure 10: Throttle input by PI controller

Now, the performance of the designed controller with  $\mu$  estimator (ASMC with  $\mu$  estimator) is compared by the controller without estimator (ASMC). To demonstrate the robustness and effectiveness of the proposed controller against the frictional uncertainties of tire forces, two kinds of simulations are carried out and compared: low and high model uncertainties (as the decrease of 20% and 30% in the tire-road friction coefficient, respectively). The simulation results for clutch engagement at standing start are illustrated in Figures 11 to 15.

The performance of the ASMC system for the clutch synchronization process is illustrated in

Figure 11. These graphs are corresponding to states of with and without the  $\mu$  estimator. It is assumed that there is 20% parametric uncertainty in the road friction coefficient. As it can be observed, the clutch lock-up time and rotational acceleration of clutch slip for the ASMC system are 0.775 s and 45 rad/s<sup>2</sup>, respectively. These values are decreased to 0.531 s and 44.5 rad/s<sup>2</sup> in the ASMC system with the  $\mu$  estimator. The results indicate that the time of clutch synchronization for ASMC with the  $\mu$  estimator is reduced significantly, by about 31.5%, compared with the ASMC system. Although, the rotational slip acceleration is almost the same in both systems and has not changed remarkably.

The estimated values of the road friction coefficient are shown in Figure 12. Figure 13 illustrates the control throttle input related to the system with 20% frictional uncertainties of tire forces until clutch lock-up. Similarly, the performance of the presented control system, in the case of reducing the road friction coefficient by 30%, can be seen in Figures 14 and 15.

As it can be found in Figure 14, the clutch lock-up time and the time derivative of clutch slip, related to the ASMC approach, are 0.913 s and 53 rad/s<sup>2</sup>, respectively. These values have been reduced to 0.533 s and 51.5 rad/s<sup>2</sup> in the ASMC system with the  $\mu$  estimator. The results indicate that the time of smooth clutch engagement for ASMC with the  $\mu$  estimator has decreased considerably, by about 41.6%, compared with the ASMC system. Again, as in the previous case, the slip acceleration has not changed significantly. The observed values of the road friction coefficient are shown in Figure 15. According to this figure, the estimated value rapidly converges from an initial value ( $\mu=0.63$ , by reduction of 30%), to the actual value ( $\mu=0.9$ ). Therefore, the effect of the ASMC- $\mu$  estimator is appreciable for the reduction in the driveline oscillations and decreasing the clutch synchronization time. A summary of the results discussed above is given in Table 2.

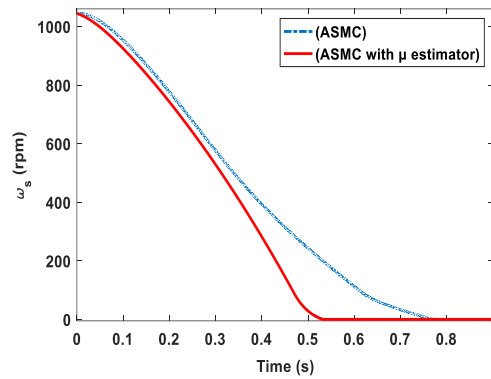
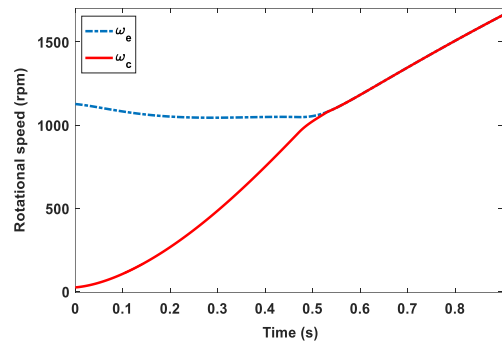
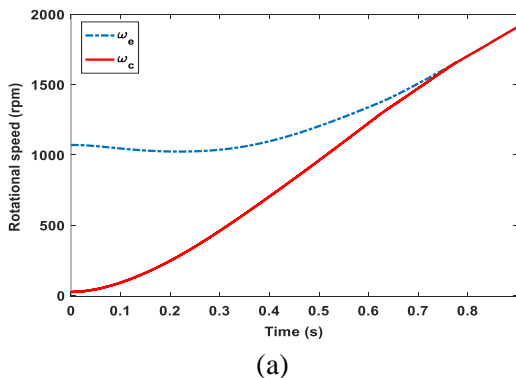


**Figure 11:** Slip speed during clutch engagement for the ASMC method in comparison with the ASMC system with  $\mu$  estimator in case of 20% uncertainties in the road friction coefficient (a):  $\omega_e$  and  $\omega_c$  of ASMC system, (b):  $\omega_e$  and  $\omega_c$  of ASMC system with  $\mu$  estimator, (C): Clutch slip speed

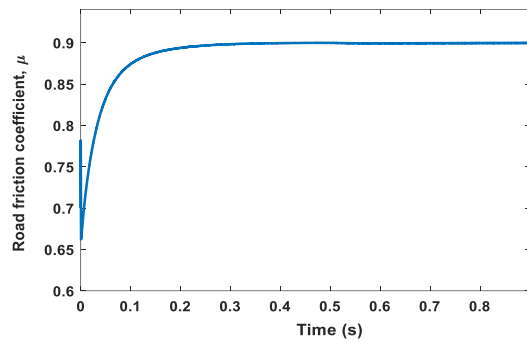


**Figure 12:** Road friction estimation result with 20% frictional uncertainties of tire forces

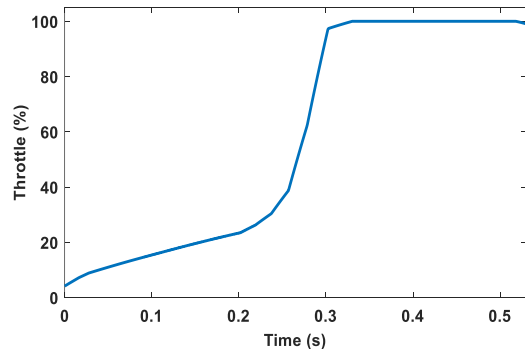
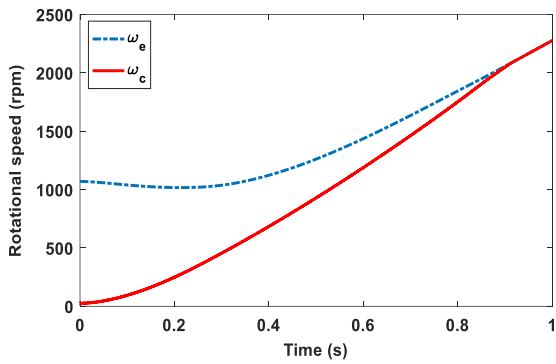
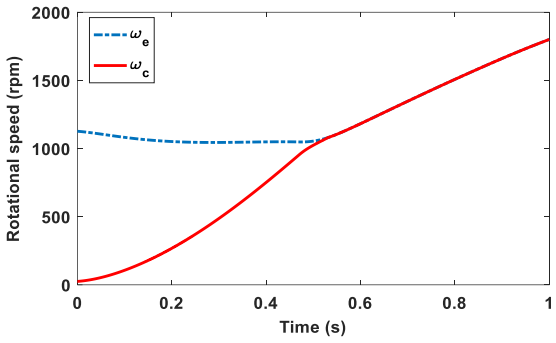


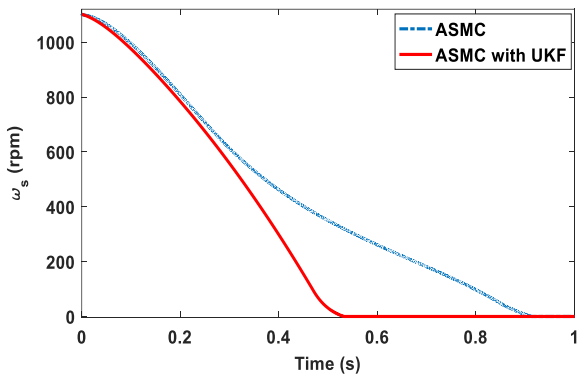
**Figure 13:** Throttle input with 20% frictional uncertainties of tire forces until clutch lock-up



(a)



(b)



(c)

**Figure 14:** Slip speed during clutch engagement for the ASMC method in comparison with the ASMC system with  $\mu$  estimator in case of 30% uncertainties in the road friction coefficient (a):  $\omega_e$  and  $\omega_c$  of ASMC system, (b):  $\omega_e$  and  $\omega_c$  of ASMC system with  $\mu$  estimator, (C): Clutch slip speed

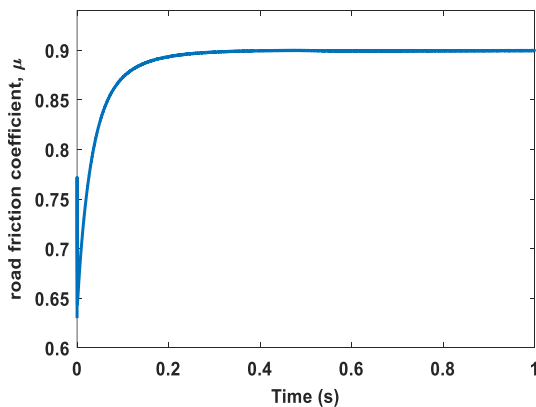


**Fig. 15:** Road friction estimation result with 30% frictional uncertainties of tire forces

**Table 2:** Comparison between the clutch lock-up time for the ASMC and the ASMC- $\mu$  estimator systems

$\mu$ Parameter uncertainties	20%		30%	
Control system	ASMC	ASMC- $\mu$ estimator	ASMC	ASMC- $\mu$ estimator
Clutch lock-up time (s)	0.775	0.531	0.913	0.533
Relative improvement of ASMC with $\mu$ estimator	31.5%		41.6%	

## 6. Conclusions

In this paper, an ASMC system based on estimation of tire-road friction coefficient was designed for smooth engagement control of automotive dry clutch. Moreover, an estimator by UKF was adopted to observe the states that are hardly measured such as tire slip ratio. Since the road friction coefficient has considerable effect on drive shaft torque, an estimator was designed to calculate this parameter based on the equations of tire model. The ASMC was designed for the clutch control to cope with the system uncertainties, and a PI controller was presented to engine speed control. It can be indicated from the simulation results that the proposed ASMC-UKF with  $\mu$  estimator is appropriate for reducing the powertrain oscillations after the clutch lock-up, decreasing the shocks during the driving, and causing faster engagement.

## References

- [1] A. Soltani, M. Arianfard, R. N. Jazar. Application of unscented Kalman filter for clutch position control of automated manual transmission. *Archive of Mechanical Engineering*, Vol. 69, No.2, (2022), pp. 319-339.
- [2] J. Horn, J. Bamberger, P. Michau, S. Pindl. Flatness-based clutch control for automated manual transmissions. *Control Engineering Practice*, Vol. 11, No. 12, (2003), pp. 1353-1359.
- [3] X. Y. Song, Z. X. Sun, X. J. Yang, G. M. Zhu. Modelling, control, and hardware-in-the-loop simulation of an automated manual transmission. *Proc. IMechE, Part D: J. Automobile Engineering*, Vol. 224, No. 2, (2010), pp. 143-160.
- [4] J. Kim, S.B. Choi. Control of dry clutch engagement for vehicle launches via a shaft torque observer. *Proceedings of the 2010 American Control Conference*, IEEE, 11509488, 2010.
- [5] J. Oh, J. Kim, S.B. Choi. Robust feedback tracking controller design for self-energizing clutch actuator of automated manual transmission. *SAE International Journal of Passenger Cars-Mechanical Systems*, Vol. 6, No. 3, (2013), pp. 1510-1517.
- [6] B. Gao, Y. Lei, A. Ge, H. Chen, K. Sanada. Observer-based clutch disengagement control during gear shift process of automated manual transmission. *Vehicle System Dynamics*, Vol. 49, No. 5, (2011), pp. 685-701.
- [7] A. Ge, H. Jin, Y. Lei. Engine constant speed control in starting and shifting process of automated mechanical transmission (AMT). No. 2000-05-0109. *SAE Technical Paper*, 2000.
- [8] P. Dolcini, H. B'échart, C. C. d. Wit. Observer-based optimal control of dry clutch engagement. *Proceedings of the 44th IEEE Conference on Decision and Control*. IEEE, 2005.
- [9] F. Garofalo, L. Glielmo, L. Iannelli, F. Vasca. Optimal tracking for automotive dry clutch engagement. *IFAC Proceedings*, Vol. 35, No. 1, (2002), pp. 367-372.
- [10] L. Glielmo, L. Iannelli, V. Vacca, F. Vasca. Speed control for automated manual transmission with dry clutch. *2004 43rd IEEE Conference on Decision and Control (CDC) (IEEE Cat. No. 04CH37601)*, 2, 2004.
- [11] Q. Niu. Clutch control during starting of AMT. *Procedia Engineering*, Vol. 7, (2010), pp. 447-452.
- [12] M. Jiang, J. Zhou, W. Chen, Y. Zhang, L. Chen. Modeling and simulation of AMT with MWorks. *Proceedings of the 8th International Modelica Conference; March 20th-22nd; Technical Univeristy; Dresden; Germany, Linköping University Electronic Press*, Vol. 63, (2011), pp. 829-836.
- [13] B. Gao, H. Chen, Y. Mac, K. Sanada. Design of nonlinear shaft torque observer for trucks with Automated Manual Transmission. *Mechatronics*, Vol. 21, No. 6, (2011), pp. 1034-1042.
- [14] J. Oh, J. Kim, S.B. Choi. Design of estimators for the output shaft torque of automated manual transmission systems. *2013 IEEE 8th Conference on Industrial Electronics and Applications (ICIEA)*, 13682806, 1370-1375, 2013.
- [15] J. Xuefeng, X. Xian, J. Guodong, C. Wei. Research on hill start control for heavy truck with AMT, *2012 International Conference on Computer Application and System Modeling*. Atlantis Press, 1169-1172, 2012.
- [16] X. Wang, L. Li, K. He, Y. Liu, C. Liu. Position and force switching control for gear engagement of automated manual transmission gear-shift process. *Journal of Dynamic Systems, Measurement, and Control*, Vol. 140, No. 8, 2018.
- [17] S. A. Haggag. Sliding mode adaptive PID control of an automotive clutch-by-wire actuator. *SAE International Journal of Passenger Cars-Mechanical Systems*, Vol. 9, No. 1, (2016), pp. 424-434.
- [18] P. Song, R. Fang, J. Dai. Coordinated engine torque and clutch control during gear-shifting process of automated manual transmission. *SAE Technical Paper*, 2018-01-0866, 2018.

[19] R. Temporelli, M. Boisvert, P. Micheau. Control of an electromechanical clutch actuator using a dual sliding mode controller: Theory and experimental investigations. *IEEE/ASME Transactions on Mechatronics*, Vol. 24, No. 4, (2019), pp. 1674-1685.

[20] A. Bagheri, S. Azadi, A. Soltani. A combined use of adaptive sliding mode control and unscented Kalman filter estimator to improve vehicle yaw stability. *Proc. IMechE, Part K: J. Multi-body Dynamics*, Vol. 231, No. 2, (2017), pp. 388-401.

[21] M. Sharifzadeh, M. Pisaturo, A. Senatore. Real-time identification of dry-clutch frictional torque in automated transmissions at launch condition. *Proceedings of the Institution of Mechanical Engineers, Part D: Journal of Automobile Engineering*, Vol. 234, No. 2-3, (2020), pp. 586–598.

[22] A. Della Gatta, L. Iannelli, M. Pisaturo, A. Senatore, F. Vasca. A survey on modeling and engagement control for automotive dry clutch. *Mechatronics*, Vol. 55, (2018), pp 63-75.

[23] D. Bhattacharjee, P. Bhola, P. K. Dan. An analytical review on automatic gear shifting in automatic transmission. *International Journal of Vehicle Design*, Vol. 77, No. 4, (2018). Pp 227-246.

[24] L. Li, Z. Zhu, X. Wang, Y. Yang, C. Yang, J. Song. Identification of a driver's starting intention based on an artificial neural network for vehicles equipped with an automated manual transmission. *Proc. IMechE, Part D: J. Automobile Engineering*, Vol. 230, No. 10, (2016), pp. 1417-1429.

[25] Dynamometer test results of EF7 engine reported by IPCO.